JOURNAL OF MATERIALS SCIENCE 36 (2001) 4239–4247

# Benefits of toughening a vinyl ester resin matrix on structural materials

P. J. BURCHILL
*Aeronautical and Maritime Research Laboratory, PO Box 4331, Melbourne 3001, Australia*

A. KOOTSOOKOS
*Department of Aerospace Engineering, RMIT University, P.O. Box 2476V, Melbourne 3001, Australia*

M. LAU
*Co-operative Research Centre for Polymers, 32 Business Park Drive, Notting Hill, Vic 3149, Australia*

A commonplace vinyl ester resin blended with a core-shell polymer additive has been used as a matrix for some typical structural commercial materials to determine the benefits of increased matrix toughness. In a simulation of polymer concrete, the tougher matrix was found to increase the toughness of the concrete by a small amount. Unexpectedly the flexural strength was increased by 30% which has been ascribed to the greater damage tolerance of the matrix. In composites with fibre glass cloth, the interlaminar toughness is also improved. An application of extreme value statistics showed that the change in resin toughness due to blending was fully transferred to the composite, and also allowed an estimation of the effect of the reinforcement on toughness.


## 1. Introduction

Toughening of polymer resins has a lengthy history [1, 2], but most of the studies with thermosets are of epoxy resins. These resins have excellent environmental resistance compared to the much cheaper unsaturated polyester resins, and many studies are driven by aerospace applications which have required a resistance to heat and moisture which polyesters are unable to offer. While certain polyesters have much better resistance towards sunlight than structural epoxies, these materials are rarely used uncoated in composite structures. The biggest need in development of these matrix resins has been to improve their properties against matrix dominated failure in composites. Reactive liquid polymers (RLPs) such as carboxy terminated butadiene-acrylonitrile co-polymers have been commonly studied additives [3–9]. More recently, core-shell polymers have been studied as toughness promoting additives in epoxy resins [10–14], though one of the first recorded uses of these materials in toughening thermoset resins was with an unsaturated polyester resin [15].

Cheaper alternatives to epoxies are vinyl ester resins which, though unsuitable for aerospace applications, are becoming increasingly considered for their good environmental resistance. Typical applications range from copper refining tanks and chemical storage vessels to casings on submarines [16]. The additives used for toughening epoxy resins are not effective with the commonplace vinyl ester resins, though there has been some success in toughening a modified vinyl ester [17–19]. Alternatively, the RLP has to be rendered more compatible with the standard vinyl ester resin [20]. Recent research in these laboratories, has shown that vinyl esters can be toughened through blending with core-shell polymers [21, 22], and the most effective of these additives were shown to have a polybutadiene core.

This current study has looked at the application of core-shell polymer toughened vinyl ester resin as a matrix for fibre reinforced composites, and as a matrix in highly filled resin simulations of polymer concrete. The use of a toughened resin in a fibre reinforced composite does not necessarily mean that the composite will be toughened to the same degree as the resin [23, 24]. An earlier study, in which RLPs were used to toughen the vinyl ester resin, showed that the improvement was conferred into a fibre-glass composite [25]. Toughened resins do not appear to have been used in polymer concrete.

## 2. Experimental

### 2.1. Materials

The vinyl ester resin, Hetron® 922, was supplied by Huntsman Chemical Company Australia, and the core shell additive was obtained from Fidene Corporation as KCA102 (Kureha). Later this additive was replaced by a chemically identical material EXL2602 (Rohm & Haas). The reinforcement was a woven roving—AR106, Colan Products Pty. Ltd., nominal areal density 630 g/m$^2$—with a vinyl ester resin compatible finish. The composition of the cloth was warp 29.5 yarns per 10 cm, 1200 tex., and weft 15.8 yarn per 10 cm,

1800 tex. The glass beads, A120 and 1922 CPO3, were obtained from Potter's Industries with nominal diameters of 1.1 mm and 200 $\mu$m respectively.

The resin and core shell additive were mixed in the ratio of 100 parts resin and 5 parts additive together with styrene (17 parts) to reduce the viscosity and aid blending. This mixture was allowed to stand for 24 h before being processed with a Silverson L4R homogeniser, using a disintegration head to disperse the additive.

Resin and blends were cured at room temperature (RT) using cobalt octoate (0.3 pphr) and methylethylketone peroxide (1.5 pphr). Gel times were adjusted with dimethylaniline (accelerator) or 2,4-pentanedione (retarder) depending upon the application. In making composites, 0.13 pphr of 2,4-pentanedione was used to give a pot life of 1.5 hours, while in the polymer concrete simulations 0.22 pphr of 2.4-pentanedione was used to give a pot life of 4 hours.

## 2.2. Composite fabrication

Composites were made in a Teflon lined mould (300 mm $\times$ 500 mm) using a vacuum bagging technique. Sixteen plies of E-glass woven roving were cut with the warp direction measuring 300 mm. Between the 8th and 9th plies of glass cloth a Teflon film de-bond layer ($\sim$100 mm $\times$ 500 mm) was placed at approximately 50 mm above the centre line of the laminate. The layup process was then continued until all 16 plies of glass were used taking extra care not to shift the position of the de-bond layer. A vacuum bag with the vacuum pump connections was next put in place and edges sealed, and vacuum was applied to approximately 80 kPa until the resin gelled. The thickness of the final laminate was varied by changing the starting time at which vacuum was applied. When a test vial of the resin had gelled the composite was kept under vacuum for a further hour before being lifted from the mould, then laid flat, and left at room temperature (RT) overnight before post-curing (90°C for 90 minutes) as required. A description of the composites is given in Table I.

## 2.3. Polymer concrete simulation

Polymer concrete was simulated by mixtures of glass beads and vinyl ester resin. Two sizes of glass beads were used: 1.1 mm and 200 $\mu$m diameters. Using the 1.1 mm beads alone, the maximum glass content achieved was 70 wt%. A glass content of 80 wt% was achieved by using a mixture of 68 wt% large beads and 32 wt% small beads, a choice guided by R. M. German's work on particle packing, and by ease of consolidation [26].

The castings were made using a 40 $\times$ 50 $\times$ 300 mm Teflon-lined cavity mould. To improve workability of the final mix, the resin was preheated. For single bead mixes the resin was first heated at 40°C for 40 minutes. The retardant and promoter were then added and the mix reheated for a further 40 minutes at 40°C. Finally, the peroxide was added to the resin, and then the glass beads were mixed in by hand. For the two bead mixes, the promoter and retardant were added to the resin and that mixture then preheated for 1.5 hours at 65°C. The beads were then mixed in by hand as before.

The consolidation process was the same for each mixture. After pouring the mixture into the mould, the mould was placed upright and fixed onto a vibrating table. Compaction of the material was achieved by vibrating the casting for two and a half hours. Gelation did not occur during compaction. The samples were left to cure overnight at room temperature, and post-cured at 90°C for 90 minutes.

After post-curing, the $K_{Ic}$ samples were notched using a radial arm saw. The starter crack, or sharpened notch, was produced by using a Leco VC-50 metallographic saw, with a diamond blade. The initial crack lengths were kept to 0.45 W.

## 2.4. Fracture resistance

Double Cantilever Beam (DCB) specimens (25 mm $\times$ 190 mm) with the long axis parallel to the warp direction

TABLE II Polymer concrete simulations

| Sample | Resin | Glass type | Glass content (wt%) |
|---|---|---|---|
| 1 | Hetron® 922 | 1.1 mm | 70 |
| 2 | Hetron® 922 | 1.1 mm, 200 $\mu$m | 80 |
| 3 | Toughened 922 | 1.1 mm, 200 $\mu$m | 80 |

TABLE I Fabricated composites

| Composite No. | Composite structure Hetron® 922, 16Plies-Woven Roving | Cure conditions |
|---|---|---|
| M2 | Glass Content : 55.65 wt% | Post-cured at 90°C for 90 mins |
| M3 | Glass Content : 59.47 wt% | Post-cured at 90°C for 90 mins |
| M4 | Glass Content : 70.76 wt% | Post-cured at 90°C for 90 mins |
| M5 | Glass Content : 63.18 wt% | Post-cured at 90°C for 90 mins |
| M6 | Glass Content : 65.80 wt% | Post-cured at 90°C for 90 mins |
| M7 | Glass Content : 70.10 wt% | RT without post-cure, aged |
| M8 | Glass Content : 66.34 wt% | RT without post-cure, aged |
| M9 | Glass Content : 66.98 wt% | RT without post-cure, aged |
| M10* | Glass Content : 66.06 wt% | Post-cured at 90°C for 90 mins |
| M11* | Glass Content : 69.17 wt% | Post-cured at 90°C for 90 mins |
| M12† | Glass Content : 69.81 wt% | Post-cured at 90°C for 90 mins |
| M13† | Glass Content : 63.81 wt% | Post-cured at 90°C for 90 mins |
| M14† | Glass Content : 76.66 wt% | Post-cured at 90°C for 90 mins |
| M15† | Glass Content : 57.80 wt% | Post-cured at 90°C for 90 mins |
| M16† | Glass Content : 63.58 wt% | RT without post-cure, aged |

*Contains 5 pphr of KCA 102.
†Contains 5 pphr of EXL 2602.

were cut from the composite panels, to have a 50 mm de-bond (Teflon film) length at one end. End tabs were adhered onto the de-bond end using M-bond 300 adhesive, taking care to align both tabs with the edge of the specimen. One side of the specimen was painted with whitener to aid observation of the crack growth and marking of the crack length. The specimen was carefully put under a tensile load to open the de-bonded zone and pre-crack to about 52 mm from the beginning. The tests were done at a crosshead speed of 2 mm/min, and when a pre-determined crosshead displacement was reached, the specimen was unloaded by about 5% of the displacement before marking the crack length. The first measurement was generally between 60 to 75 mm from the open end of the beam. The computer recorded the corresponding load and displacement before the unloading. Generally, about 12 measurements were recorded. The direction of crack growth relative to the cloth structure was along the warp.

These results were analysed by two methods, one due to Hashemi, Kinloch and Williams [27] and another due to Rosensaft [28]. Both methods of data reduction gave essentially the same values for fracture toughness and the values reported here are from analysis using equations derived by Hashemi *et al.*

For each specimen the compliance was calculated from:

$$C = 8N\frac{(a+\chi h)^3}{Bh^3E_{11}} \quad (1)$$

$N$ is a correction factor which accounts for the stiffening effects of the attachments required to load the specimen and corrections due to large displacements and attachment tilting, other symbols are: crack length $a$, thickness $2h$, width $B$, modulus $E_{11}$. The term $\chi h$, adjusts the compliance due to the measured crack length with compliance of the un-cracked part of the specimen [27, 29, 30].

Strain energy release rate was calculated from:

$$G_1 = (F/N)\cdot 3P\delta/2B(a+\chi h) \quad (2)$$

$F$ is a factor which corrects for the shortening of the crack length due to large displacements, the other symbols are: load $P$, and displacement $\delta$. Equations for $F$ and $N$ can be found in reference [27] and [30].

Fracture toughness of the simulated polymer concrete was measured using single edge notched bar specimens ($40 \times 50 \times 200$ mm). The fracture toughness of the polymer concrete material was determined using single-edge notch samples ($40 \times 50 \times 200$ mm), tested in three-point bending. The critical $K$ value, $K_{Ic}$, was determined from the plateau region of the R-curve as described in ASTM E561-94 [31]. During testing, the crack opening displacements (COD) were measured using a clip gauge attached to the sample by knife edges. COD values were then converted to crack lengths by the calibration curve presented by Willoboughy and Garwood [32]. Three R-curves were determined for each composition and at least two estimates of $K$ were made from each curve.

Flexural properties of the polymer concrete were measured in three point bending according to an ASTM standard [33]. As the samples were not of a standard geometry, the strain-rate used for testing was determined according to the formula laid out in the standard. Three flexural tests were performed for each composition.

## 3. Results and discussion

### 3.1. Polymer concrete

The glass content of the polymer concrete simulation was varied deliberately to assess the effects of glass content and bead diameter on toughness. The standard resin and the toughened vinyl ester resin were used as matrix materials, to see if having a tougher matrix affected the properties of the resulting composite. Toughness was determined from notched three point bend specimens, and the value of $K_{Ic}$ determined from R-curves. Fig. 1 gives the curves obtained for all the specimens using toughened resin, and the critical value was estimated from the plateau region of the curves. Table III summarises the results from the toughness measurements, and the flexural property experiments.

Previous research has mainly concentrated on developing an understanding of the compressive properties

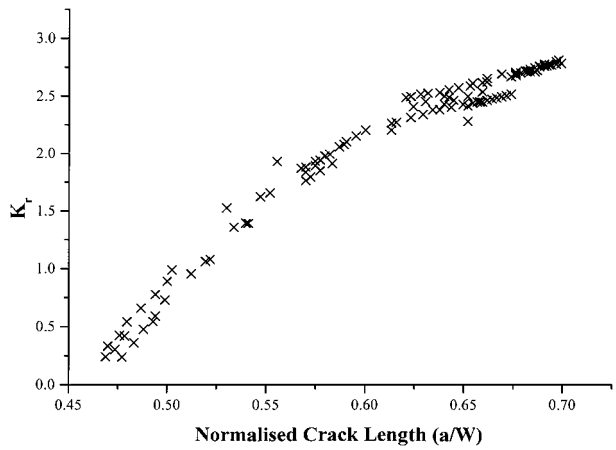


*Figure 1* R-curve data for polymer concrete Mix 3.

TABLE III Toughness, modulus and bend strength results for polymer concrete

| Material | Composition | $K_{Ic}$ (MPa$\sqrt{m}$) | $\sigma$ (MPa) | $E$ (GPa) | $G$ (Jm$^{-2}$) |
|---|---|---|---|---|---|
| Mix 1 | Plain resin + 70 wt% glass | $1.36 \pm 0.4$ | $17.5 \pm 1.1$ | $7.75 \pm 0.67$ | 240 |
| Mix 2 | Plain resin + 80 wt% glass | $2.3 \pm 0.99$ | $18.8 \pm 0.9$ | $10.73 \pm 0.5$ | 490 |
| Mix 3 | Toughened resin + 80 wt% glass | $2.7 \pm 0.13$ | $25.5 \pm 0.9$ | $7.55 \pm 0.18$ | 960 |

of polymer concrete. Typically, the matrix resin used is an unsaturated polyester, although there has been some work done on particulate filled epoxies [34–36]. In terms of fracture toughness, a limited amount of data is available. Dharmarajan and Vipulanandan [37] examined the effect of filler content on the toughness of a polyester mortar. They found that $K_{Ic}$ increased from 0.6 MPa$\sqrt{}$m to 1.2 MPa$\sqrt{}$m with an increasing amount of resin in the mortar, over the resin weight percentages of 10–18%. For this composition range they developed a linear relationship between $K_{Ic}$ and the flexural strength measured in four-point bending. In contrast, Andouni and Sautereau *et al.* [38] examined the effects of filler content on the mechanical properties of rubber-toughened epoxies and they found that for composites up to 28 volume percent filler, there was an optimum filler content which maximized the fracture toughness. Similarly, Moloney *et al.* [39] also found that $K_{Ic}$ was optimized at a specific volume fraction of filler for coated beads, while for composites containing uncoated beads, $K_{Ic}$ increased linearly with increasing volume fraction of filler.

The fracture toughness results (Table III) indicate that increasing the glass content also increases the fracture toughness, consistent with the findings of Moloney *et al*. [39]. Use of a toughened resin for the matrix phase also produced an increase in toughness.

It is interesting to note that the scatter in the $K_{Ic}$ results for the toughened resin composite is much less than that of the composite made using the plain resin. This reduction in scatter may be a result of the fact that the plain resin exhibits stick-slip cracking behaviour, while the toughened resin does not. Thus, for the plain resin, the $K_{Ic}$ results are an average of crack initiation and crack propagation $K$ values. Examination of the fractures surfaces of the 80 wt% glass composites (mixes 2 and 3) shows that the failure mode of the toughened resin is different to that of the standard resin (see Figs 2 and 3). The plain resin shows "riverline" fracture typical of brittle materials, while the toughened resin exhibits some form of deformation. The increase in toughness produced by using the toughened resin is no doubt related to this change of fracture surface. The differences in the crack propagation of the two resins would also be related to the different fracture surfaces observed.

Consideration of the flexural strength results shows that use of a toughened resin also increases the breaking strength. Comparison of these results with similar mechanical properties of the neat resins (Table IV) shows that polymer concrete materials exhibit a large reduction in strength. This reduction is no doubt due to the presence of the filler acting as a stress concentrator. Nevertheless, the ratio of the toughened neat resin strength to the toughened polymer concrete mixture is higher than the same ratio for the untoughened resin. A clear indication that even though the toughened resin has a lower strength than the neat resin, it produces, proportionally, a much stronger composite. This effect may arise because the increased ductility of the toughened resin accommodates the stress concentrations produced by the filler, thereby allowing the composite to withstand higher loads. The different crack propagation modes of the two resins support this idea.

While results in the literature generally quote flexural strengths of the same order of magnitude as the results considered here, the flexural moduli vary greatly.

TABLE IV Vinyl ester resin matrix flexural properties

| Resin | Yield strength (MPa) | Flexural modulus (GPa) | Toughness ($Jm^{-2}$) | Ratio of concrete strength to resin strength |
|---|---|---|---|---|
| Plain | 133 | 3.12 | 180 | 0.14 |
| Toughened | 107 | 2.81 | 2080 | 0.24 |

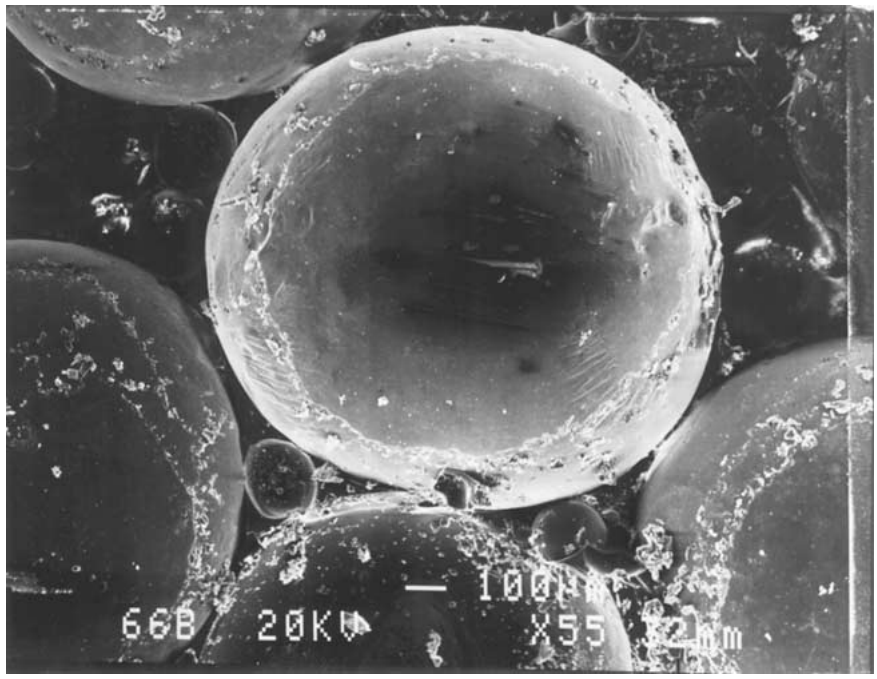


*Figure 2* Fracture surface of polymer concrete with plain resin (Mix 2).

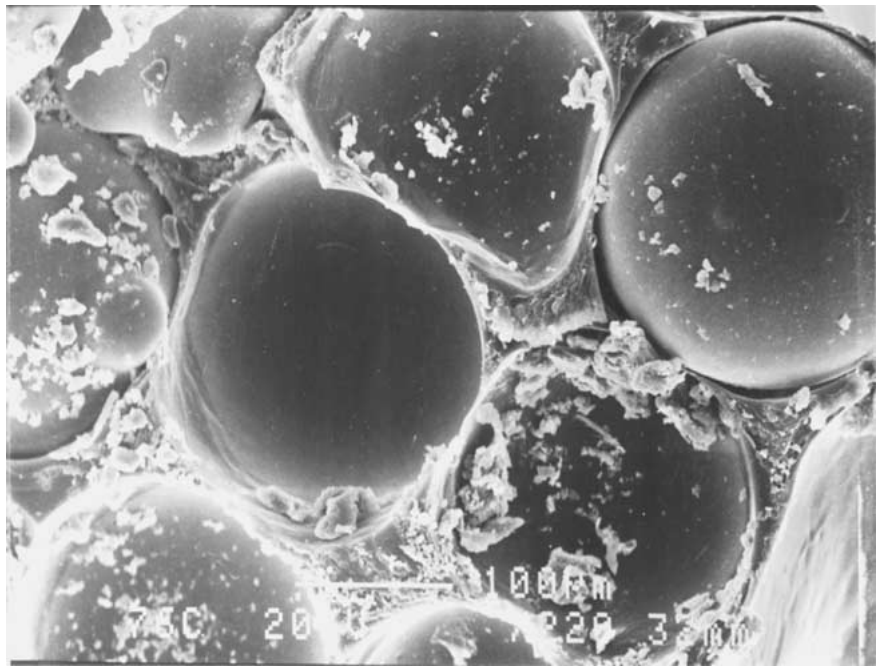

*Figure 3* Fracture surface of polymer concrete with toughened resin.

Dharmarajan and Vipulanandan [37] quote values between 1 and 4 GPa and other sources quote values between 3 and 20 GPa. The sources quoting the higher values used silica as a reinforcing agent [39–41].

In the present case, the toughened resin composite had a reduced flexural modulus compared to the untoughened resin composite. It is possible that the reduction in modulus of the toughened composite is due to the rubber toughening agent in the matrix phase, however, the modulus measured in flexure is much smaller than what would be expected from the Rule of Mixtures [42]. The modulus is also much less than that calculated as a lower bound modulus from the equation due to MacDonald and Ransley [43, 44],

$$1/E = 1/E_1 f + 1/E_2(1 - f) \qquad (3)$$

which gave, for example, values of 19 GPa and 18 GPa respectively for the plain and toughened resin concretes for the 80%wt fraction ($f = 88.5$ vol%), taking the modulus of the glass beads as 69 GPa. Thus, it can probably be stated that the low values of modulus observed here, and by others, must indicate that bonding between the resin and the filler is extremely poor.

## 3.2. Fibre-glass composites

Because of the difficulty in making fibre reinforced resin composites by wet lay-up with a known, reproducible fibre volume fraction, fracture toughness measurements were made on composites in which the fibre content was deliberately varied. In addition, the effect of cure on the composites has also been assessed, with some composites only receiving a room temperature cure and aging while other have been post-cured at 90°C for 90 minutes. For each composite panel at least seven specimens were tested, and from each specimen generally 12 measurements of load, displacement and crack length were obtained.

### 3.2.1. Method of analysing double cantilever beam data

The first step in determining the strain energy release rate, G, from the load, displacement and crack length measurements, is estimation of the adjustment $\chi h$ in Equation 1. This adjustment was found to vary widely from specimen to specimen for each composite, and to assume both negative and positive values. Negative values are explained as compliance of the specimen ahead of the crack tip [29], whilst the explanation offered for positive values is fibre bridging to give the appearance that the actual crack length is less than that measured [46]. The method adopted here has been to pool all the data from the specimens tested of one panel, by normalising the compliance, and deriving a common $\chi h$. Fig. 4 shows a typical plot of $(CBh^3/N)^{1/3}$ against crack length, and contains usually 80 or more separate measurements.

Table V gives values of $\chi h$ found for each composite panel, and the calculated modulus $E_{11}$ the error in which was less than 1 GPa. Application of Equation 2 with the global value of $\chi h$ for the panel gave the tabled average values of the strain energy release rate $G$ and their standard deviations.

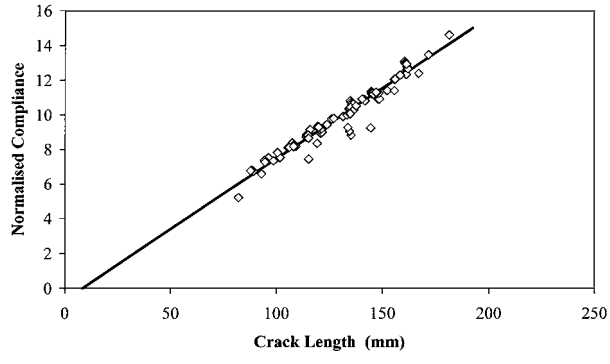


*Figure 4* Cube root of normalised compliance data plotted against crack length for all the specimens tested from panel M5.

TABLE V Summary of results from fracture measurements on composite panels

| Panel | Glass content (wt%) | $\chi h$ (mm) | $\chi h$, error (mm) | Modulus ($E11$) (GPa) | $G$ ($Jm^{-2}$) | $G$, error ($Jm^{-2}$) |
|---|---|---|---|---|---|---|
| M2 | 55.65 | −14.1 | 5.2 | 21.9 | 532 | 209 |
| M3 | 59.47 | −6.3 | 2.6 | 25.2 | 328 | 89 |
| M4 | 70.76 | −11.2 | 2.3 | 23.1 | 604 | 194 |
| M5 | 63.18 | 8.3 | 2.9 | 14.8 | 461 | 168 |
| M6 | 65.80 | 0.2 | 2.0 | 19.5 | 435 | 184 |
| M7 | 70.10 | 5.6 | 1.5 | 20.5 | 1231 | 218 |
| M8 | 66.34 | 6.7 | 1.5 | 17.0 | 1043 | 278 |
| M9 | 66.98 | 6.2 | 1.2 | 16.6 | 1204 | 344 |
| M10 | 66.06 | 5.0 | 0.8 | 16.9 | 2067 | 194 |
| M11 | 69.17 | −0.2 | 0.9 | 21.5 | 1994 | 189 |
| M12 | 63.81 | 2.1 | 1.0 | 20.1 | 2544 | 254 |
| M13 | 63.81 | −3.8 | 0.8 | 20.6 | 1923 | 193 |
| M14 | 76.66 | 3.1 | 1.1 | 22.4 | 2428 | 289 |
| M15 | 57.80 | 6.0 | 1.0 | 13.2 | 2087 | 295 |
| M16 | 63.58 | 1.6 | 0.9 | 17.9 | 2468 | 320 |

### 3.2.2. Fibreglass composite properties

For these calculated average values of $E_{11}$ and $G$ there appears to be no correlation with the glass content of the panels. The average modulus also shows a much greater spread between panels than the average $G$ values despite the accuracy with which each is determined. Panels with a lower value of $E_{11}$ seem to have more positive $\chi h$ values, but low values of $E_{11}$ would mean that for a measured compliance the crack length is smaller than expected, implying higher toughness which is not the case. Hence the difference between panels may lie in the difficulty in determining the actual crack length. This measurement is constrained to the edge of the specimen, but within the specimen the true crack front is unknown. A penetrating dye indicated that the crack front is fairly linear and normal to the edge given the waviness of the fibre bundles. Another factor, which contributes to the scatter in the values of $E_{11}$, is the assumption that the plane of the crack coincides with the geometric centre. However, even for those specimens in which the two arms are not the same thickness, the increase in compliance due to this effect is insufficient to explain a lower modulus. If the thinner beam were two-thirds the thickness of the other, the apparent reduction in modulus due to assuming the same thickness would be only about 20%. In addition, low modulus specimens did not correspond with the greatest mismatch in beam thicknesses.

The experimental procedure adopted to determine the toughness of the fibre glass composites and to determine the effect of increase in resin toughness arose because of the unstable nature of the crack growth. Composites with the untoughened resin showed stick-slip crack growth, though even between arrest points there was some slow growth. Hence, the estimations of strain energy release rate are averages lying between the catastrophic initiation values and the arrest values. Crack growth behaviour in composites with the toughened resin was not so erratic. Analysis of the individual $G$ values determined from each specimen from a panel showed no correlation with either position along the specimen or location of the specimen within the panel so indicating that these were not the source of error in the estimations. In addition, an analysis of variance of the measurements from any panel showed that all the specimens are not the same. While there are small variations in specimen thickness there was no correlation with the specimen toughness. Aside from crack length measurement, this experimental scatter may be due to variations in:

Local resin thickness between the plies along the crack plane,
Amount of fibre bridging or enmeshing between plies,
Amount of glass in the specimen parallel to the major axis,
Void content along the crack plane,
Crack deflection as it follows the weave, and
Crack plane not being on the central axis.

Occasionally, cracking which will also contribute to the toughness is seen in the next interlaminar zone parallel to the main crack on the edge of the specimen at the crack front.

The four fold increase obtained in the average toughness of those composites in which the resin is toughened (Table V, M10–M15) is similar to published results on woven reinforcement composites with epoxy resins and vinyl ester resins, where a liquid rubber toughening additive was used [24, 25]. Results obtained using the core-shell additive KCA102 or its replacement, EXL2602, are indistinguishable. The results also show that the dependence of toughness on glass content is small over the content range 55–75 wt% with some suggestion that toughness increases with content. Composites with un-toughened resin which were not post-cured appear to have a toughness about twice those that are fully cured, though the effect of cure condition with toughened resin appears to be more moderate.

Interlaminar fracture toughness of woven roving composites is not determined solely by resin toughness. In unidirectional composites the effect of fibres in increasing toughness is described as being due to fibre bridging which results in energy absorption from fibre fracture and fibre pull out [24, 45, 46]. Fibre bridging is probably less important in woven roving composites

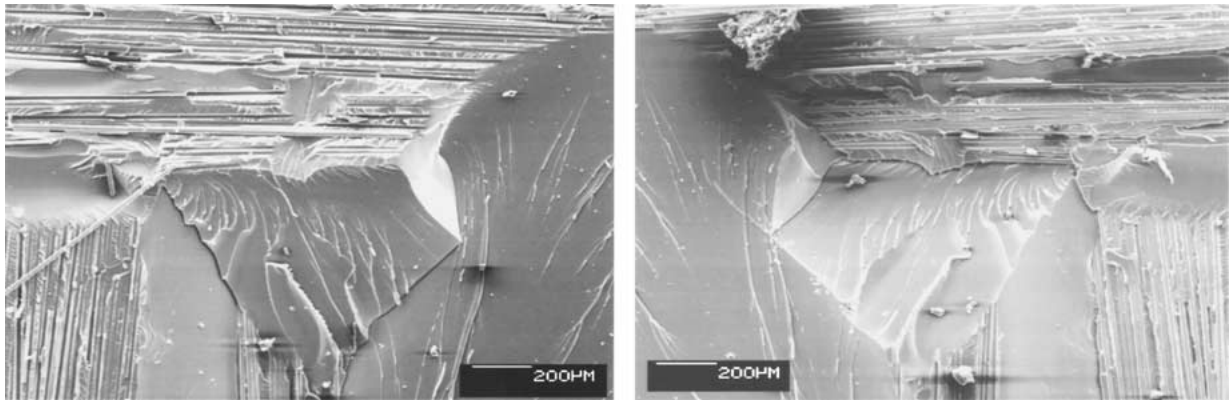


*Figure 5* Fracture surface of composite with plain resin showing matching regions on opposite sides of the crack.

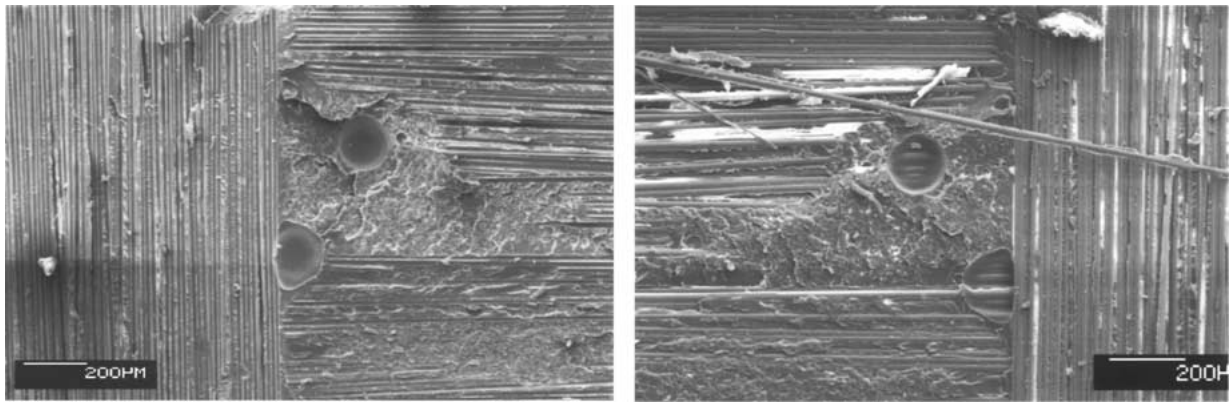


*Figure 6* Fracture surfaces of composite with toughened resin showing matching regions and how the crack path follows the weave and penetrates into the yarns.

since fracture surfaces do not show extensive filament breakage. However, the fracture surface, especially in the toughened resin composites, is not always normal to the load direction since the crack front follows the weave of the cloth. Weft fibre bundles also show that the growing crack penetrates the bundle and is not simply deflected around. Both effects would result in a much greater surface area being created during cracking than might have been expected. Deflection would introduce a mode II component into the toughness, also contributing to larger values since mode II failure requires more energy than mode I. Figs 5 and 6 are composite fracture surfaces showing how with the toughened resin, the crack follows more closely the surface of the cloth.

In estimating the value of interlaminar fracture toughness of these composites it is clear that there is a large amount of scatter in the data which can be seen graphically in Fig. 7. In this figure, all the toughness values for all the specimens from panels M2–M6 and M10–M15 have been plotted against individual specimen thickness, which is a measure of the resin content. Clearly, the dependence of toughness on glass content is very weak for these composites. The large scatter hides the effectiveness that toughening the resin contributes to interlaminar fracture toughness, and shows that the reinforcement contributes a highly variable proportion of the energy required for crack growth. To determine if the benefits for toughening can be rendered more apparent, order statistics has been applied to the results.

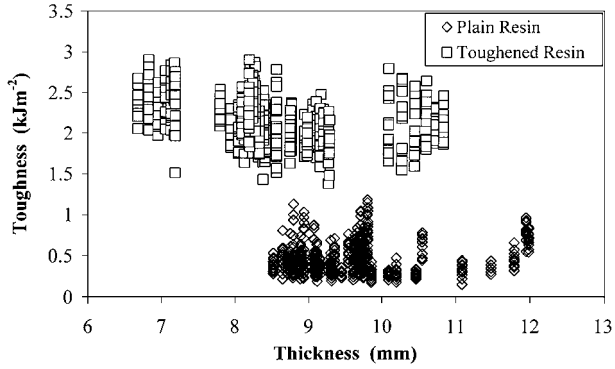


*Figure 7* Calculated fracture toughness values plotted against specimen thickness for post-cured plain and toughened resin composites.

### 3.2.3. Application of order statistics to composite data

While the results show that for average values of $G$, the tougher resin will give a tougher composite, the use of averages especially where stick-slip is observed is open to question. Composites with the toughened resin showed a lesser tendency for stick-slip and so the improvement to initiation values for crack growth may be quite different. Therefore, the individual values of $G$ for each experimental measurement have been analysed by order statistics [47, 48]. The maximum value recorded for each specimen is an approximation of the energy required for initiation of crack growth. Assuming also that glass content has negligible effect for the

TABLE VI Analysis of composite toughness ($Jm^{-2}$)

| Composite matrix | Cure conditions | Composite toughness (Largest maximum) | Composite toughness (Smallest maximum) | Toughness donated by glass fibres | Change in largest maximum from post-cure | Change in smallest maximum from post-cure |
|---|---|---|---|---|---|---|
| Untoughened | RT + 90°C | 1150 | 300 | 850 | −910 | −840 |
| Untoughened | RT | 2060 | 1140 | 920 | | |
| Toughened | RT + 90°C | 2920 | 2020 | 900 | −640 | −520 |
| Toughened | RT | 3560 | 2540 | 1020 | | |

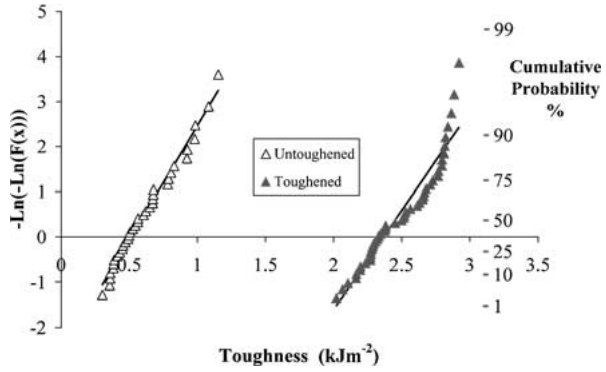


*Figure 8* Extreme value probability plot of the maximum toughness measurements from individual specimens for post-cured composite plates with plain and toughened resin matrixes, $F(x) = i/(1+n)$.

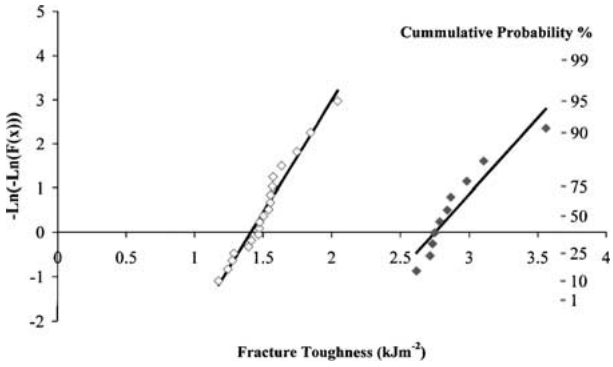


*Figure 9* Extreme value probability plot of the maximum toughness measurements from individual specimens for room temperature cured composite plates with plain and toughened resin matrixes, $F(x) = i/(1+n)$.

range studied, then the results for the same matrix and cure history can be pooled. Fig. 8 displays probability plots for observing fracture energies at or less than a specified value and derived from the maximum values observed for each specimen from panels M2–M6, and M10–M15. The function $F(x)$ is $i/(n+1)$ where $n$ is the number of largest observations and $i$ is the position in the ordering of these observations. This treatment of the data is an analysis of the distribution of the extreme values obtained from each specimen. The linear plot shows that the distributions of largest values are similar to the Gumbel distribution or Type 1 asymptotic distribution of largest extremes. Fig. 9 displays similar plots for composite panels which were not post cured, M7–M9, and M16. The offset between the curves in each figure is very similar to the increase in resin toughness when it is blended with the core-shell polymer, and complements previously published work on toughening vinyl ester resin composites with reactive liquid polymers [25]. These results clearly indicate that improvements to resin toughness are more fully transferred to composites than might be expected from other studies [23, 24].

### 3.2.4. Contributions of the reinforcement and post-cure to toughness

Assuming that in the distribution of largest values, the smallest of these values are determined by the toughness of the resin, and the largest are determined by resin and contributions due to the fibre bridging then the energy involved in fibre pull-out and fracture may be estimated. Crack growth in these composites is a mixture of stick-slip and continuous, and these largest values can reasonably be considered to be a measure of crack growth initiation. Table VI gives the overall smallest and the largest values for crack initiation representing resin alone and resin plus fibre toughness. The results for the four sets of composites indicate that the reinforcement contributes from 0 to 900 $Jm^{-2}$ towards the energy requirement for initiation.

The effect of post-curing the resin appears to have a large effect on the toughness of a composite with the unmodified resin. This effect is probably due to the fact that thermal shrinkage stresses do not develop within the room temperature cured composite. An estimate of the size of the effect of post curing on toughness is also shown by the extreme values and is shown in Table VI. For un-toughened resins post-curing appears to lower the composite toughness by about 870 $Jm^{-2}$ while with the toughened resin the reduction is less at about 580 $Jm^{-2}$ which may be due to easier stress relief in the more ductile resin.

## 4. Conclusions

While toughening of a matrix resin can be achieved in a variety of ways, this improvement is not necessarily conferred upon its composites. Through the use of vinyl ester resin blended with a core shell polymer additive as a matrix the results show that toughening by this route is beneficial. For polymer concrete, not only is the material toughness enhanced, but the flexural strength is also increased significantly probably due to the greater ductility in the matrix accommodating stress concentrations due to the filler. In fibre glass composites, the increased toughness of the matrix is fully transferred to interlaminar toughness. These observations show that using a matrix, which is also biphasic during fabrication

of these structural materials will cause no difficulties, and that it is not necessary that the matrix be homogeneous before cure commences.

## References


1. C. B. BUCKNALL, "Toughened Plastics" (Applied Science, London, 1977).
2. A. A. COLLYER, "Rubber Toughened Engineering Plastics" (Chapman & Hall, London, 1994).
3. R. S. DRAKE and W. J. McCARTHY, *Rubber World* **159**(1) (1968) 51.
4. E. H. ROWE, A. R. SIEBERT and R. S. DRAKE, *Mod. Plast.* **47** (1970) 110.
5. J. N. SULTAN and F. J. McGARRY, *Polym. Eng. Sci.* **13** (1973) 29.
6. A. C. MEEKS, *Polymer* **15** (1974) 675.
7. L. T. MANZIONE, J. K. GILLHAM and C. A. McPHERSON, *J. Appl. Polym. Sci.* **26** (1981) 907.
8. S. WU, *Polym. Int.* **29** (1992) 229.
9. R. BAGHERI and R. A. PEARSON, *Polymer* **37** (1996) 4529.
10. P. C. YANG, E. P. WOO, M. T. BISHOP, D. M. PICKELMAN and H. J. SUE, *PMSE* **63** (1990) 315.
11. H. J. SUE, *J. Mater. Sci.* **27** (1992) 3098.
12. H. J. SUE, E. I. GARCIA-MEITIN and N. A. ORCHARD, *J. Polym. Sci. Part B, Polym. Phys.* **31** (1993) 595.
13. F. LU, H. H. KAUSCH, W. J. CANTWELL and M. FISCHER, *J. Mater. Sci. Lett.* **15** (1996) 1018.
14. G. LEVITA, A. MARCHETTI and A. LAZZERI, *Makromol. Chem. Macromol. Symp.* **41** (1991) 179.
15. R. A. DICKIE and R. A. PETT, US Patent 3,652,722 (1972).
16. P. J. BURCHILL and P. J. PEARCE, in "Polymeric Materials Encyclopedia," edited by J. C. Salamone (CRC Press, New York, 1996) p. 2204.
17. I. GRABOVAC, P. J. PEARCE and A. W. CAMILLERI, *IUPAC Int. Symp. Polym.* **91** (1991) 202.
18. J. S. ULLETT and R. P. CHARTOFF, *Polym. Eng. Sci.* **35** (1995) 1086.
19. E. DREERMAN, M. NARKIS, A. SIEGMANN, R. JOSEPH, H. DODIUK and A. T. DIBENEDETTO, *J. Appl. Polym. Sci.* **72** (1999) 647.
20. S. PHAM and P. J. BURCHILL, *Polymer* **36** (1995) 3279.
21. P. J. BURCHILL, SON PHAM and M. LAU, unpublished results.
22. K. ROBERTS, P. J. BURCHILL, G. SIMON and W. COOK, to be published.
23. W. D. BASCOM, J. L. BITNER, R. J. MOULTON and A. R. SIEBERT, *Composites* **11** (1980) 9.
24. D. L. HUNSTON, *Compos. Technol. Rev.* **6** (1984) 176.
25. P. J. BURCHILL and G. J. SIMPSON, in Proceedings of ICCM-11, edited by M. L. Scott (1997) Vol. II, p. II-254.
26. R. M. GERMAN, "Particle Packing Characteristics" (Metal Powder Industries Foundation, Princeton, USA, 1989).
27. S. HASHEMI, A. J. KINLOCH and J. G. WILLIAMS, *Proc. Royal Soc.* **A427** (1990) 173.
28. M. ROSENSAFT and G. MAROM, *J. Comp. Tech. Res.* **10** (1988) 114.
29. M. F. KANNINEN, *Int. J. Fracture* **9** (1973) 83.
30. J. G. WILLIAMS, *J. Strain Anal.* **24** (1989) 207.
31. Annual Book of ASTM Standards, Vol. 03.01, ASTM E561-94, "Standard practice for R-Curve Determination."
32. ANTHONY A. WILLOUGHBY, STEPHEN J. GARWOOD, in Elastic-Plastic Fracture: Second Symposium, Fracture resistance Curves and Engineering Applications, ASTM STP 803, edited by C. F. Shih and J. P. Gudas (American Society of Testing and Materials) Vol. II, p. II-372.
33. Annual Book of ASTM Standards, Vol 08.01, D790M-86, "Standard Test Method for Flexural properties of Unreinforced and Reinforced plastics and Electrical Insulating Materials."
34. WEI-HWANG LIN, MING-HWA R. JEN and FU-SIN TZEN, in Proceedings of the National Services Council, Republic of China, Part A: Physical Science and Engineering (1995) Vol. 19, No. 6, p. 582.
35. C. VIPULANANDAN, *Polym. Eng. and Sci.* **29** (1989) 1628.
36. *Idem., J. Appl. Polym. Sci.* **41** (1990) 751.
37. N. DHARMARAJAN and C. VIPULANANDAN, *ibid.* **42** (1991) 601.
38. N. AMDOUNI, H. SAUTEREAU, J. F. GERARD, F. FERNAGUT, G. COULON and J. M. LEFEBVRE, *J. Mater. Sci.* **25** (1990) 1435.
39. A. C. MOLONEY, H. H. KAUSCH, T. KAISER and H. R. BEER, *J. Mater. Sci.* **22** (1987) 381.
40. J. X. LI, M. SILVERSTEIN, A. HILTNER and E. BAER, *J. Appl. Polym. Sci.* **52** (1994) 255.
41. S. MEBARKIA, C. VIPULANANDAN, *Polym. Eng. and Sci.* **34** (1994) 1287.
42. WILLIAM D. CALLISTER JR., "Materials Science and Engineering: An Introduction" (John Wiley and Sons, Inc, New York, 1985) p. 399.
43. N. F. MACDONALD and C. E. RANSLEY, Special Report No. 58 of the iron and Steel Institute of London, 1954.
44. B. PAUL, *Trans. Metall. Soc. AIME* **218** (1960) 36.
45. X. N. HUANG and D. HULL, *Compos. Sci. Technol.* **35** (1989) 283.
46. J. M. SLEPETZ and L. CARLSON, in "Fracture Mechanics of Composites," ASTM Special Technical Pub. **593** (1975) 143.
47. E. J. GUMBEL, 'Statistics of Extremes,' Columbia University Press, New York (1966).
48. N. R. MANN, R. E. SCHAFER and N. D. SINGPURWALLA, "Methods for Statistical Analysis of Reliability and Life Data" (John Wiley and Sons, New York, 1974).



*Received 17 March 2000*
*and accepted 13 April 2001*